Journal of
Applied Crystallography
ISSN 0021-8898

Received 16 August 2006
Accepted 6 February 2007

Wide-q observation from 10^{-4} to 2.0 Å^{-1} using a focusing and polarized neutron small-angle scattering spectrometer, SANS-J-II

Hiroki Iwase,[a] Satoshi Koizumi,[a]* Jun-ichi Suzuki,[b] Takayuki Oku,[b] Hajime Sasao,[b] Hirokazu Tanaka,[a] Hirohiko M. Shimizu[b,c] and Takeji Hashimoto[a]

[a]Advanced Science Research Center, Japan Atomic Energy Agency, Tokai, Ibaraki 319-1195, Japan, [b]Quantum Beam Science Directorate, Japan Atomic Energy Agency, Tokai, Ibaraki 319-1195, Japan, and [c]RIKEN, Wako, Saitama 351-0198, Japan. Correspondence e-mail: koizumi.satoshi@jaea.go.jp

In order to extend an upper q-limit [q is the magnitude of the scattering vector **q**, defined by $q = (4\pi/\lambda)\sin\theta$, where λ and 2θ are the wavelength and the scattering angle, respectively], high-angle ^{3}He sub-detectors were installed on a focusing and polarized neutron small-angle scattering spectrometer (SANS-J-II) at JRR-3, Tokai, Japan. Consequently, the upper q-limit was improved from 0.2 to 2.0 Å^{-1}. To quantitatively discriminate spin incoherent scattering from hydrogen or to perform nuclear spin polarization contrast variation, a remanent supermirror analyser is also available on the high-angle sub-detector. By combining a focusing ultra-small-angle scattering, realised by compound and/or magnetic lens and high-resolution area detector, SANS-J-II is able to cover from 3×10^{-4} to 2.0 Å^{-1} (*four orders of magnitude of q*), which benefits investigation of hierarchically ordered systems, found widely in hard, soft and bio-materials.

1. Introduction

In this paper, we report our challenge on 'wide length scale observation from Å to μm', overcoming the q-limitation of the conventional reactor small-angle neutron scattering (SANS) spectrometer, where q is the magnitude of the scattering vector **q**, defined by $q = (4\pi/\lambda)\sin\theta$ (λ and 2θ are the wavelength and the scattering angle, respectively). After reconstruction of the reactor SANS spectrometer SANS-J at JRR-3, Tokai, using advanced neutron devices and additional area detectors, the new spectrometer, named SANS-J-II, extends the accessible q-region by *one order of magnitude lower and higher*. Consequently, SANS-J-II covers four orders of magnitude from 10^{-4} to 2.0 Å^{-1}.

Fig. 1, showing small-angle scattering from a polymer gel [poly(*N*-isopropylacrylamide) (PNIPA)] swollen in D_2O (Koizumi *et al.*, 2004), emphasizes the accessible q-region and differential scattering cross section ($d\Sigma/d\Omega$) before our reconstruction. The ultra-small-angle range of 10^{-5} Å^{-1} covered by double crystal ultra-small-angle neutron scattering (USANS) spectrometer PNO at JRR-3, Tokai, is also shown.

As the solution temperature increases around $T = T_v$ (= 307.5 K) at which an abrupt change in volume (or volume phase transition) happens. Small-angle scattering from the PNIPA gel changes dramatically; below T_v, there is Ornstein–Zernike type scattering from thermal concentration fluctuations in the PNIPA gel, whereas above T_v, the collapsed PNIPA chains due to cooperative dehydration in a single chain form solid-like domains with a sharp interface boundary dispersed in the D_2O rich matrix (Koizumi *et al.*, 2004). Above T_v, $d\Sigma/d\Omega$ is sufficient for double crystal USANS, whereas

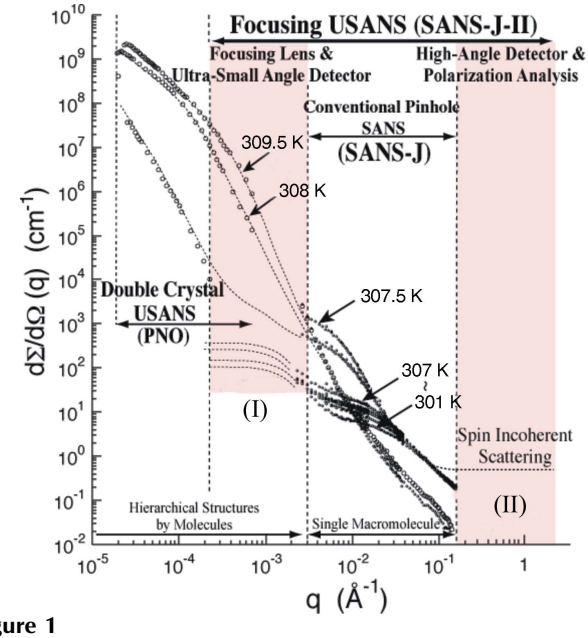

Figure 1
Accessible q-regions from a conventional pinhole SANS spectrometer (SANS-J) and a double crystal USANS spectrometer (PNO), indicated by scattering curves obtained for poly(*N*-isopropylacrylamide) swollen gel in D_2O with different solution temperatures.

because of lack of luminosity, double crystal USANS hardly reaches to small $d\Sigma/d\Omega$ less than 10^3 cm^{-1}, which corresponds to the thermal concentration fluctuations in a swollen gel. Thus there is an invisible area in the ultra-small-angle scattering (USAS) region, as indicated by (I) in Fig. 1. To cover this USAS region, a focusing collimation is utilized (Koizumi *et al.*, 2006)

There is another inaccessible q-region at high-q, because of spin incoherent scattering [marked as (II) in Fig. 1]. Most soft materials, including bio-materials, are composed of organic compounds containing a large number of hydrogen atoms. Therefore, spin incoherent scattering is strong enough, appearing as a background in high-q region ($q > 0.1$ Å^{-1}), where coherent small-angle scattering asymptotically decays according to $q^{-\alpha}$ (for example, α is close to 2 or 4 for a random coil or interfacial structures). In order to overcome this problem, we aim to perform neutron polarization analysis to quantitatively discriminate spin incoherent scattering. By using the polarization analysis with a spin ^{3}He filter, trial experiments for separating coherent and incoherent scattering were demonstrated on the NG3 SANS instrument at NIST (Gentile *et al.*, 2000).

2. Focusing and polarized neutron small-angle scattering spectrometer (SANS-J-II)

The conventional pinhole SANS spectrometer SANS-J at research reactor JRR-3 has been operated since 1991. In reconstruction towards SANS-J-II, we did not change the following instrument bases from those of SANS-J: (i) total spectrometer length (20 m); (ii) velocity selector (providing wavelength λ from 3.0–20 Å with $\Delta\lambda/\lambda$ = 0.08–0.3, and transmission of neutron $T = 0.75$) and (iii) ^{3}He Risø-type two-dimensional position sensitive detector. Consequently, SANS-J-II is able to cover the conventional q-region accessed by SANS-J ($3 \times 10^{-3} < q < 0.2$ Å^{-1}).

To perform a wide q-range observation from 10^{-4} Å^{-1} to 2.0 Å^{-1}, we constructed the following three items; (i) a 'T-shape collimator' with focusing and polarizing devices, (ii) a high-angle ^{3}He sub-detectors with a spin analyzer at sample position, and (iii) a high-resolution area detector in front of the main ^{3}He area detector. The construction (i) and (iii) was crucial to approach the USAS region of 10^{-4} Å^{-1} order, which is referred to in Koizumi *et al.* (2006). The construction of (ii), on the other hand, is crucial to approach the high-q observation up to 2.0 Å^{-1}. After these constructions, SANS-J was successfully modified to the focusing and polarized neutron small-angle scattering spectrometer, SANS-J-II [Fig. 2(*b*)].

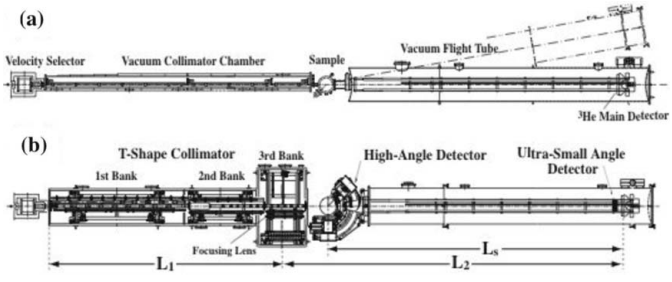

Figure 2
Schematic views for (*a*) conventional pinhole SANS spectrometer (SANS-J) and (*b*) focusing and polarized neutron ultra-small-angle scattering spectrometer (SANS-J-II) (Koizumi *et al.*, 2006).

2.1. High-angle ^{3}He detectors

To access high-q up to $q = 2.0$ Å^{-1}, we installed high-angle ^{3}He sub-detectors 1 and 2; these ^{3}He area detectors were provided by ORDELA Co. Ltd and have 250×250 mm^2 sensitive area and 2.5 mm resolution. Fig. 3(*a*) shows the high-angle detectors, installed at the sample position. Sample-to-detector distance is 0.95 m. Because of geometrical restrictions against a vacuum flight tube, the high-angle detector 1 covers from scattering angle 2θ = 23.5–57.5° on the left-hand side, with respect to a primary beam, whereas the high-angle detector 2 covers from 2θ = 23.5–98° on the right-hand side. When we choose incident neutron of $\lambda = 4$ Å, the high-angle detector 1 can cover from 0.7 Å^{-1} to 1.5 Å^{-1}, whereas the

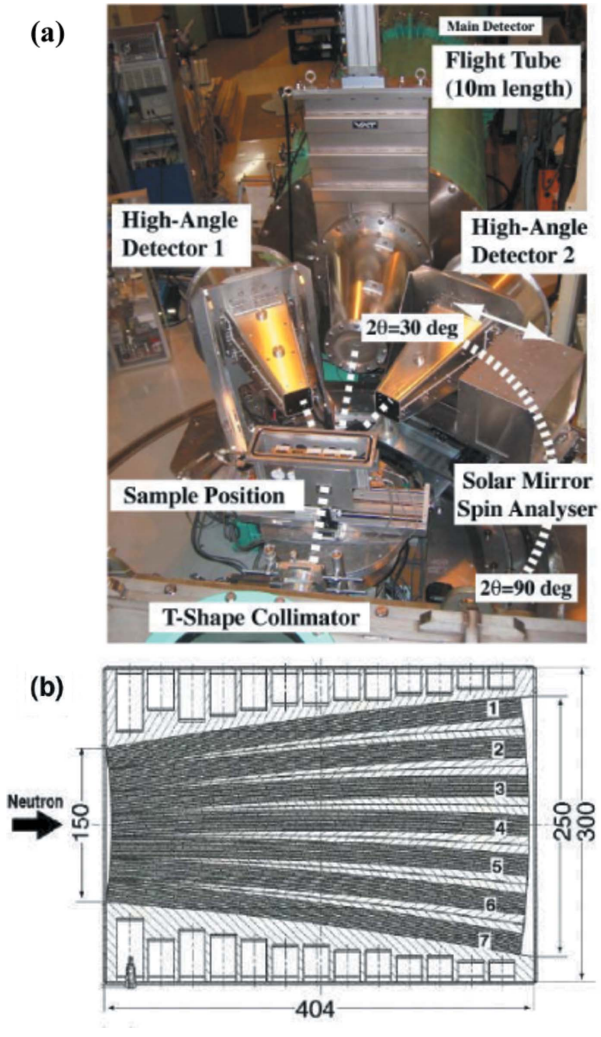

Figure 3
(*a*) Photo of high-angle ^{3}He detectors on SANS-J-II. With a remanent spin analyzer, installed in front of the high-angle ^{3}He detector, polarization analysis is available. (*b*) Schematic diagram of remanent supermirror spin analyzer.

high-angle detector 2 can cover from 0.7 Å^{-1} to 2.4 Å^{-1}. In order to perform polarization analysis, the high-angle detector 2 has a spin analyzer, which is composed of 70 sheets of curved borosilicate glass substrates (0.3 mm) where the concave and convex surfaces are coated with remanent supermirror (FeCoV/TiNx) with different reflection quality (Qc = 1.5 and 2.5 m, respectively), as schematically shown in Fig. 3(*b*). The spin analyser is able to slide into a beam position [see Fig. 3(*a*)]. According to polarization measurements on the MORPHEUS spectrometer at SINQ, Paul Scherrer Institute, Villigen, Switzerland, the polarization for the spin analyzer was 0.94. Polarized neutron beam is provided by a supermirror (Fe/Si), which is installed in the T-shape collimator. In order to polarize neutrons of full-width and height (20 × 50 mm^2), we set a long supermirror of 2.5 m, which is inclined at 0.46° with respect to a primary beam direction. The transmission polarized beam is transmitted by magnetic guide field of 10 Gauss. For the polarization analysis, we utilize two coil, Drabkin type π-flippers allocated in the middle of collimator or radio-frequency (RF) π-flippers located at sample position.

3. Results

3.1. Ultra-small-angle scattering of 10^{-4} A^{-1}

Fig. 4 shows USANS measurements on an irradiated Al specimen, which contains voids of R_g = 224 Å. Double crystal USANS spectrometer PNO at JRR-3 covers USAS region of 3 × 10^{-5} Å^{-1} to 10^{-3} Å^{-1}. The USANS observed at q < 10^{-3} Å^{-1} might be due to heterogeneous spatial distributions of the voids in the specimen. On the other hand, conventional pinhole SANS, which is available on SANS-J-II, covers the q-region from 3 × 10^{-3} Å^{-1} to 2 × 10^{-2} Å^{-1} by employing with sample-to-detector distance L_s = 10.2 m. Focusing USANS experiments were performed on SANS-J-II, using a biconcave compound (MgF_2) lens (Koizumi *et al.*, 2006; Eskildsen *et al.*, 1998, Choi *et al.*, 2000) with first and sample aperture sizes of 2.5 mm × 2.5 mm and 20 mm diameter, respectively. To focused neutrons with λ = 6.65 Å at L_s = 9.6 m, where the lens is allocated at nearly symmetric position L_1 = L_2 = 10 m, we needed 70 pieces of the biconcave lenses. With the focused beam, whose diameter is about 2 mm at half-height, and a high-resolution position-sensitive photomultiplier (0.5 mm resolution) coupled with ZnS/^{6}LiF scintillator, SANS-J-II successfully covers the medium USAS region from 4 × 10^{-4}Å^{-1} to 4 × 10^{-3} Å^{-1}, which corresponds to the gap between double crystal USANS and conventional pinhole SANS. It should be denoted that the focusing USANS is able to access low dΣ/dΩ (= 10^2–10^3 cm^{-1}).

3.2. High-angle scattering from 0.1 to 2.0 A^{-1}

Fig. 5 shows the scattering profiles obtained for folded sheet nano-porous silica material (FSM-16), which has honeycomb-shaped channel structures, as schematically illustrated in insert of Fig. 5. With the ^{3}He main-detector of pinhole SANS, employing two sample-to-detector distances (10.2 and 2.5 m), we were able to cover 3 x 10^{-3} < q < 0.15 Å^{-1}. At q = 0.16 Å^{-1}, we observed the first scattering maximum due to a lattice factor of the honeycomb structure. To reach to higher q, up to 2.0 Å^{-1}, the high-angle detectors 1 and 2 were necessary. To continuously cover a high q region up to q = 2.0 Å^{-1}, we needed to change detector angles several times (15°, 30°, 45°, 60°, 75°, 90°). In the high q-region up to 2.0 Å^{-1}, we observed higher scattering maxima ($\sqrt{3}$, $\sqrt{4}$, and $\sqrt{7}$) due to a lattice factor of the honeycomb structure. The solid line in Fig. 5 is a scattering curve obtained by time-of-flight small/wide-angle neutron scattering spectrometer (SWAN) at the spallation neutron source facility, High Energy Accelerator Research Organization, Tsukuba, Japan (Otomo *et al.*, 1998, 2003). SWAN is able to simultaneously cover the whole q ranges from 0.01 to 20 Å^{-1}. The scattering profiles detected by the

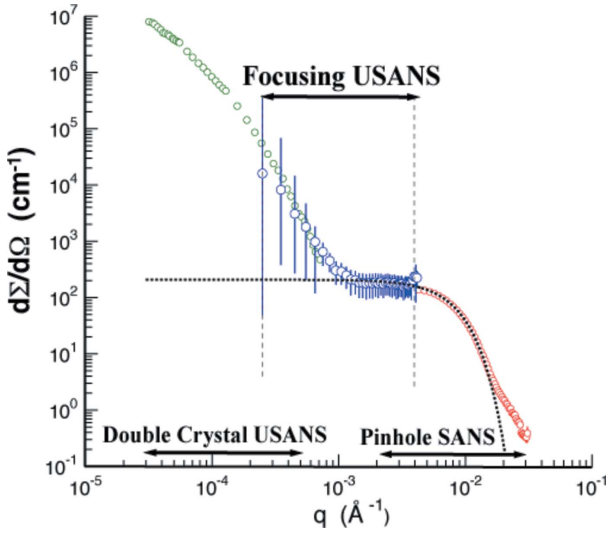

Figure 4
Scattering profiles for secondary standard of irradiated Al containing voids (Al-7).

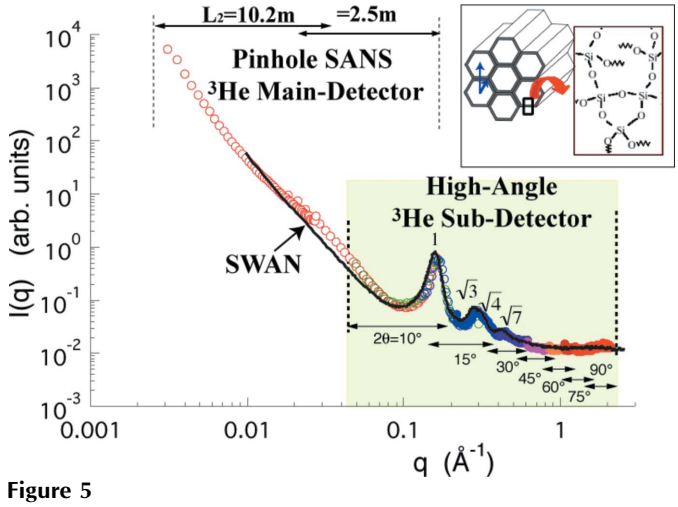

Figure 5
Scattering profiles for folded sheet nano-porous silica material (FSM-16). Preliminary results observed by high-angle sub-detectors of SANS-J-II. The solid line is a scattering profile obtained by time-of flight small/wide-angle neutron scattering spectrometer (SWAN) at KEK, Tsukuba, Japan.

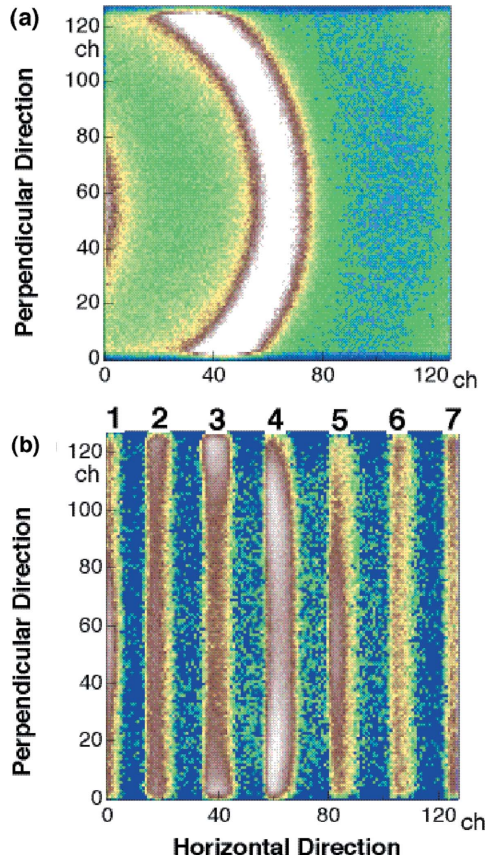

Figure 6
Two-dimensional image of scattering for FSM-16 detected by a high-angle ^{3}He detector (*a*) without spin analyzer and (*b*) with one at $2\theta = 10^\circ$. The Debye–Scherrer ring originates from the honeycomb structure of FSM-16.

high-angle detector with changing detector angles are consistent with those by SWAN.

For polarization analysis, a solar remanent supermirror is able to slide in front of high-angle detector 2. Fig. 6 shows a two-dimensional image of scattering from FSM-16. High-angle detector 2 was set at $2\theta = 10^\circ$, which corresponds to the q-region of first scattering maximum ($q = 0.16$ Å^{-1} shown in Fig. 5) of the honeycomb nano-structure. Fig. 6(*a*), without a spin analyzer, clearly shows a so-called Debye–Scherrer ring, originating from the honeycomb structure. In Fig. 6(*b*) with a spin analyzer set in front of high-angle detector 2, two-dimensional image, passing through the spin analyzer, is distorted stripe-like by the solar mirror; 7 stripes correspond to 7 branches of mirrors, as schematically shown in Fig. 3(*b*). Even with the distortion by the spin analyser, we recognize that the Debye–Scherrer ring due to the first scattering maximum remains in from the 2nd to 4th stripe, with which we are able to reproduce the q-profile originating from the honeycomb structure of FSM-16.

4. Conclusion

A conventional pinhole SANS spectrometer SANS-J was successfully reconstructed to be a focusing and polarized neutron small-angle scattering spectrometer (SANS-J-II) with a wide q-region from ultra-small-angle scattering of 10^{-4} Å^{-1} to high q of 2.0 Å^{-1}.

The authors would like to acknowledge N. Niimura (Ibaraki University) for installing high-angle ^{3}He sub-detectors, S. Sato (KENS) for data acquisition developed by using a VME CPU board, Y. Fukushima for providing sample specimens (FSM-16), T. Otomo for measurement at SWAN, M. Nagao (ISSP) for test measurement on polarization analysis and H. Yasuoka (JAEA) for financial support. Part of activities were supported under the project for development and application of neutron optical devices, founded by the Ministry of Education, Japan.

References

Choi, S.-M., Barker, J. G., Glinka, C. J., Cheng, Y. T. & Gammel, P. L. (2000). *J. Appl. Cryst.* **33**, 793–796.
Eskildsen, M. R., Gammel, P. L., Isaacs E. D., Detlefs, C., Mortensen, K. & Bishop, D. J. (1998). *Nature*, **391**, 563–566.
Gentile, T. R., Jones, G. L., Thompson, A. K., Barker, J. G., Glinka, C. J., Hammouda, B. & Lynn, J. W. (2000). *J. Appl. Cryst.* **33**, 771–774.
Koizumi, S., Iwase, H., Suzuki, J., Oku, T., Motokawa, R., Sasao, H., Tanaka, H., Yamaguchi, D., Shimizu, H. M. & Hashimoto, T. (2006). *Phys. B*, **385–386**, 1000–1006.
Koizumi, S., Monkenbusch, M., Richter, D., Schwahn, D. & Farago, B. (2004). *J. Chem. Phys.* **121**, 12721–12732.
Otomo, T., Furusaka, M., Satoh, S., Itoh, S., Adachi, T., Shimizu, S. & Takeda, M. (1998). *J. Phys. Chem. Solids*, **60**, 1597–1582.
Otomo, T., Iwase, H., Mori, K., Masui, T., Satoh, S. & Furusaka, M. (2003). KENS Report-XIV 2001–2002, pp. 32–34.